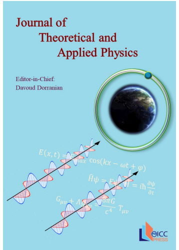


Volume 17, Issue 2, 172321 (1-8)

Journal of Theoretical and Applied Physics (JTAP)

https://dx.doi.org/10.57647/j.jtap.2023.1702.21

# Numerical investigations of electron-self-injection in different shaped bubbles in wakefield acceleration

Sonu Kumar[1], Dhananjay K. Singh[2], Hitendra K. Malik[1]*

[1] *Plasma Waves and Particle Acceleration Laboratory, Department of Physics, Indian Institute of Technology Delhi, New Delhi, India.*
[2] *Department of Physics, PKRM College, BBM Koyalanchal University, Dhanbad, India.*

***Corresponding author**: hkmalik@physics.iitd.ac.in

Received 3 October 2022; Accepted 15 November 2022; Published online 19 November 2022

**Abstract:**
Electron-self-injection in bubble wakefield acceleration is the new concept for acceleration of electrons inside bubble. In this technique, self-injected plasma electrons have been used for acceleration whose advantage is that there is no need of external source of electrons. In our case, we have carried out numerical investigations of self-injected plasma electrons in different shaped bubbles such as spherical, longitudinal ellipsoid and transverse ellipsoid bubble. For these numerical investigations, by carrying out relativistic Hamiltonian analysis of plasma electrons, we have used 4$^{\text{th}}$ order Runge-Kutta (RK) method by employing MATLAB ode45, a nonstiff differential equations solver. We have discussed different parameters such as impact parameter, radius of bubble, bubble velocity for their effect on the formation of bubbles with different shapes and self-injection of the electrons.

**Keywords:** Bubble wakefield acceleration; Plasma; Impact parameter; Bubble velocity; Bubble radius

## 1. Introduction

Accelerated charged particles with very high velocity comparable to the light speed, when collide with other moving particles or stationary target, create a huge amount of energy. Today, Large Hadron Collider called as LHC accelerate charged particles in circular track and allow them collide with other charged particles. Sometimes ago, Big-bang concept was tried to be achieved in LHC laboratory for creating the condition of birth of our universe with the help of accelerator concept. Hence, new dimensions of research are possible based on the concept of particle acceleration that has other applications in fusion energy, synchrotron radiation production, nuclear energy, medical treatment and many more. However, such accelerators are huge in size and have very high cost. For example, LHC occupies 27 km of circumference, and its maintenance cost is very high involving a lot of manpower too. The conventional accelerators employ a radiofrequency cavity and have an electrical breakdown problem that limits their efficiency. For removal of such disadvantage, researchers have used the concept of wakefield acceleration, thanks to our pioneer researchers Tajima and Dawson who conceived this acceleration technique. Tajima and Dawson [1] in 1979 created an oscillatory wake in the plasma by introducing electromagnetic field driver called intense short laser pulse; specifically they generated an electron plasma wave corresponding field to which was called wakefield. This wakefield had an advantage of producing three times more accelerator gradient than the one achieved in conventional particle accelerators. Here plasma is used as a medium because it is ionized and is already in breakdown stage. In comparison to size and cost of conventional accelerators, it takes only a few meters in size and has a low cost. For the understanding point of view of the wakefield, the example of a surfer is the best example that uses the wake created by a moving boat in the lake for moving forward. One can visualize the plasma as lake, laser pulse as a driver, and the surfers as charged particles.

In the concept of laser wakefield acceleration (LWFA) [2–4], plasma electrons are expelled by energetic laser photons, creating an electron free region (a region of almost stationary ions). The expelled electrons move back to their positions because of the restoring force due to background ions and overshoot there initial positions because of their inertia and create an electron plasma wave [5]. The frequency

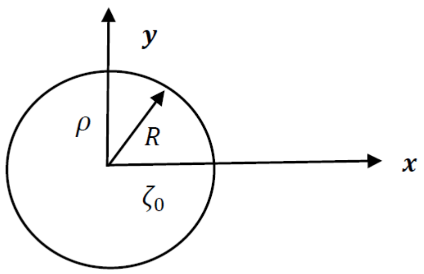


**Figure 1.** This figure shows the parameters related with bubble and $R=\sqrt{\zeta_0^2+\rho^2}$ is bubble radius, where $\zeta_0$ and $y_0=\rho$ are longitudinal and transverse coordinates.

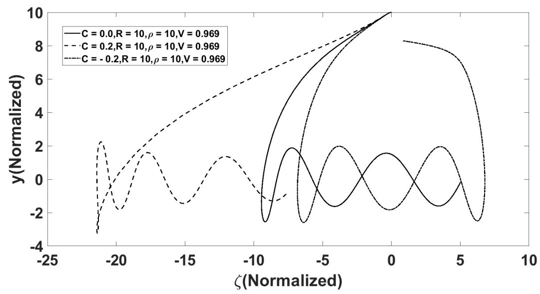


**Figure 2.** Trajectory of electrons with variation of shapes of the bubble with $C=0$ (spherical bubble), $C=-0.2$ (transverse ellipsoid bubble) and $C=0.2$ (longitudinal ellipsoid bubble) when $p_{x0}=0$, $p_{y0}=0$, $\zeta_0=\sqrt{R^2-y_0^2}$, $y_0=\rho=10$ and bubble velocity $V=0.969$ for Lorentz factor $\gamma_0=4$. Here radius of the bubble $R=10$.

of this wave is in the range of electron plasma frequency and accelerator gradient is in GeV/m. There are other methods also for the particle acceleration; for example, the plasma wakefield acceleration (PWFA) where a beam of charged particles drives the wakefield, self-modulated laser wakefield acceleration (SMLWFA) where the laser pulse gets self-modulated and the plasma beat wave wakefield acceleration (PBWA) where two laser beams drive the wakefield [6–9]. Some other wakefield acceleration techniques are their such as proton driven wakefield [10]. In LWFA, a nonlinear plasma wave is generated when the laser's intensity is quite high, and here a multidimensional wake is created, expelled plasma electrons are trapped around the boundary of the electron free region, i.e. the ion-cavity or the bubble [11–15]. Advantage of this type of wakefield acceleration is that there is no need of externally injected electrons for witness bunch. These electrons are trapped in the first wake at the tail of the bubble and self-injected into the bubble [16–18]. Self-injection of the plasma electrons in bubble wakefield is recent development for the generation of high quality electrons beam [19–28]. These high quality electron beam has been used for many applications such as material characterization [29], generation of synchrotron radiations such as betatron radiations which have been used in medical treatments [30–35] and many more [36–46].

Kostyukov et al. [47] and Lu et al. [14] have developed the model of bubble wakefield and used the spherical shape of the bubble with bubble velocity equal to one. They used a scalar gauge condition and wakefield potential with relativistic Hamiltonian equations analysis, but they did not give the concept of different shapes of bubble during self-injection of the electrons. Trajectory of the plasma electrons has been developed by Lu et al. [48] and bubble structure has been evaluated by Toosi et al. [49]. Li et al. [50] worked for the shape of the bubble by using the electromagnetic field produced inside the bubble and introduced a geometrical parameter $n$ such that $n=1$ defined the spherical bubble and $n>1$ defined the transverse ellipsoid bubble and $n<1$ defined the longitudinal ellipsoid bubble. Further work was done by Kumar et al. [17] on different gauges in bubble wakefield acceleration. But no investigation has been done numerically revealing the self-injection process of the plasma electrons and longitudinal and transverse phase-spaces in different shaped bubble regime along with a role of impact parameter, bubble radius and bubble velocity. In the present work, hence, we consider different shapes of the bubble and discuss the phenomenon concerning the electron-self-injection inside the bubbles. We deal with slower as well as faster bubble velocities on the trajectory of the trapped electrons. Our analysis with consideration of the impact parameter defines the radial distance between the trapped electrons and the laser driver.

## 2. Numerical investigation

We have considered Maxwell's equations and solved the d'Alembert differential equations by using Gauge condition $A_x=-\phi$ and wakefield potential $\Psi=A_x-\phi$. Finally, we obtain

$$\Psi=\left(\frac{1}{4}-C\right)\zeta^2+\frac{y^2}{4} \tag{1}$$

where $C$ is the geometrical coefficient, a parameter, defining the shape of the bubble. We consider space-time distribution [17] of the electromagnetic field inside the different bubbles (2D) with propagation direction $\zeta=x-Vt$, where $V$ is the bubble velocity; the transverse direction is along $y$-axis. We carry out Hamiltonian analysis [51] of the trapped electrons as $H=\sqrt{1+p_x^2+p_y^2}-VP_x-\phi$, where $P_x$ and $P_y$ are longitudinal and transverse canonical momenta of the electrons and $p_x$, $p_y$ be the longitudinal and transverse kinetic momenta of the electrons. $\gamma=\sqrt{1+p_x^2+p_y^2}$ is the relativistic Lorentz factor of the electrons. $p_x=P_x+A_x$ and $p_y=P_y$, $A_x$ and $\phi$ represents the functions of $(\zeta,y)$ and $A_\perp=0$. $\phi$ is normalized with $m_ec^2/e$, $\mathbf{A}$ is normalized with $m_ec^2/e$, where $m_e$ is the mass of electron. $\phi$ and $\mathbf{A}$ are scalar and vector potentials of the electromagnetic field. Time is normalized with $1/\omega_p$ and the length by $c/\omega_p$.

Equation of motion of the trapped plasma electrons inside the bubble (cavity) is determined by Hamiltonian equations of motion.

$$\frac{dP_x}{dt}=-\frac{\partial H}{\partial x}\frac{dP_y}{dt}=-\frac{\partial H}{\partial y},\ \frac{d\zeta}{dt}=\frac{\partial H}{\partial P_x},\ \frac{dy}{dt}=\frac{\partial H}{\partial P_y} \tag{2}$$

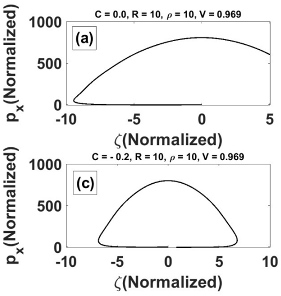


**Figure 3.** Longitudinal phase-space diagram of trapped electrons in different shaped bubble with $C = 0$ for spherical bubble (a), with $C = 0.2$ for longitudinal ellipsoid bubble (b) and with $C = -0.2$ for transverse ellipsoid bubble (c), when $V = 0.969$ for $\gamma_0 = 4$ with impact parameter of the trapped electron as $\rho = 10$ and radius of the bubble as $R = 10$.

$$\frac{dp_x}{dt} = -\frac{1}{2}(1+V)\frac{\partial \Psi}{\partial \zeta} + \frac{p_y}{2\gamma}\frac{\partial \Psi}{\partial y} \tag{3}$$

$$\frac{dp_y}{dt} = -\frac{1}{2}\frac{\partial \Psi}{\partial y} - \frac{p_x}{2\gamma}\frac{\partial \Psi}{\partial y} \tag{4}$$

$$\frac{d\zeta}{dt} = \frac{p_x}{\gamma} - V \tag{5}$$

$$\frac{dy}{dt} = \frac{p_y}{\gamma} \tag{6}$$

Now putting the expression (1) in (3) and (4), we find

$$\frac{dp_x}{dt} = -(1+V)\left(\frac{1}{4} - C\right)\zeta + \frac{p_y}{2\gamma}\frac{y}{2} \tag{7}$$

$$\frac{dp_y}{dt} = -\frac{y}{4} - \frac{p_x}{2\gamma}\frac{y}{2} \tag{8}$$

Now final four coupled differential equations are

$$\frac{dp_x}{dt} = -(1+V)\left(\frac{1}{4} - C\right)\zeta + \frac{p_y}{2\gamma}\frac{y}{2} \tag{9}$$

$$\frac{dp_y}{dt} = -\frac{y}{4} - \frac{p_x}{2\gamma}\frac{y}{2} \tag{10}$$

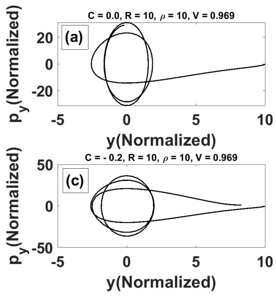


**Figure 4.** Transverse phase-space diagram of the trapped electrons in different shaped bubble when $C = 0$ (spherical bubble) in (a), $C = 0.2$ (longitudinal ellipsoid bubble) in (b) and $C = -0.2$ (transverse ellipsoid bubble) in (c) $V = 0.969$ for $\gamma_0 = 4$ with impact parameter of the trapped electron as $\rho = 10$ and radius of the bubble as $R = 10$.

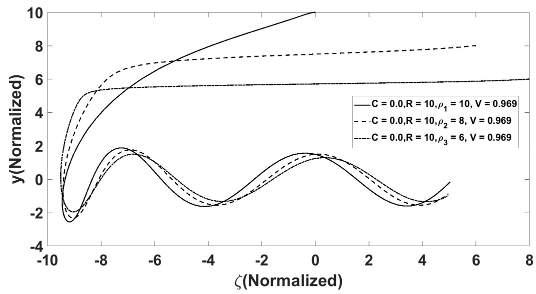


**Figure 5.** Trajectory of the electrons in spherical bubble at $C = 0$ and with initial electrons momentum value $p_{x0} = 0$, $p_{y0} = 0$, $\zeta_0 = \sqrt{R^2 - y_0^2}$, and $V = 0.969$ for Lorentz factor $\gamma_0 = 4$. Here radius of the bubble is $R = 10$ with different values of impact parameter $y_0 = \rho$.

$$\frac{d\zeta}{dt} = \frac{p_x}{\gamma} - V \tag{11}$$

$$\frac{dy}{dt} = \frac{p_y}{\gamma} \tag{12}$$

## 3. Results and discussion

Above four coupled differential equations are solved using fourth order Runge-Kutta method by using ode45 MATLAB numerical method. Here we use initial conditions as $p_{x0} = 0$, $p_{y0} = 0$, $\zeta_0 = \sqrt{R^2 - \rho^2}$, $y_0 = \rho$, where $\rho$ is an impact parameter called the radial distance between the electrons and laser pulse. For under-dense plasma, initial value of Lorentz factor depends on the bubble velocity that is $V = 1 - 1/2\gamma_0^2$ [15] which is equal to the laser pulse group velocity. Bubble radius and impact parameter have been defined in Figure 1.

### 3.1 Shape of the bubble

We have used wake potential of the generated bubble via equation (12). Hence,

$$\Psi = \left(\frac{1}{4} - C\right)\zeta^2 + \frac{y^2}{4} \tag{13}$$

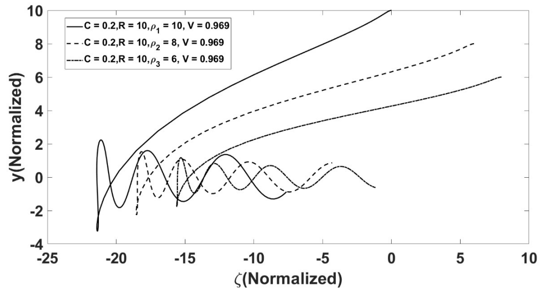


**Figure 6.** Trajectory of the electrons in longitudinal ellipsoid bubble at $C = 0.2$ and with initial electrons momentum value $p_{x0} = 0$, $p_{y0} = 0$, $\zeta_0 = \sqrt{R^2 - y_0^2}$, and $V = 0.969$ for Lorentz factor $\gamma_0 = 4$. Here radius of the bubble is $R = 10$ with different values of impact parameter $y_0 = \rho$.

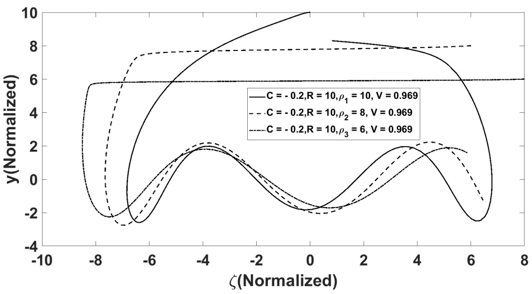


**Figure 7.** Trajectory of the electrons in transverse ellipsoid bubble at $C = 0.2$ and with initial electrons momentum value $p_{x0} = 0$, $p_{y0} = 0$, $\zeta_0 = \sqrt{R^2 - y_0^2}$, and $V = 0.969$ for Lorentz factor $\gamma_0 = 4$. Here radius of the bubble is $R = 10$ with different values of impact parameter $y_0 = \rho$.

The values of geometrical coefficient $C$ vary from $-0.2 \leq C \leq 0.2$. When $C = 0$, we get spherical bubble, at $C = 0.2$, we get longitudinal ellipsoid bubble and at $C = -0.2$, we get transverse ellipsoid bubble and these investigations on bubble shape has been already carried out by Kumar et al. [17]. Now Hamiltonian analysis of the trapped electrons is carried out with bubble velocity $V = 0.969$, i.e. slower than the speed of light, impact parameter $\rho = 10$ and radius of the bubble as $R = 10$. Here we consider different values of $C$ for the trajectory of the trapped electrons, and longitudinal and transverse phase-space portrait.

### 3.2 Trajectory of self-injected plasma electrons in different shaped bubble

Self-injection scheme of the plasma electrons has been understood by finding trajectory of these electrons in $(\zeta, y)$ direction following the process developed by Lu et al. [48] but they did the work only for spherical bubble regime. So, we have extended their work and found the trajectory in different shaped bubble as shown in Figure 2. We have found the trajectory of the self-injected plasma electrons with different shaped bubble such as spherical bubble regime at $C = 0$, longitudinal ellipsoid bubble regime at $C = 0.2$ and transverse ellipsoid bubble at $C = -0.2$. The results show that the electrons in transverse ellipsoid retrace their path greater than with the cases of longitudinal ellipsoid and

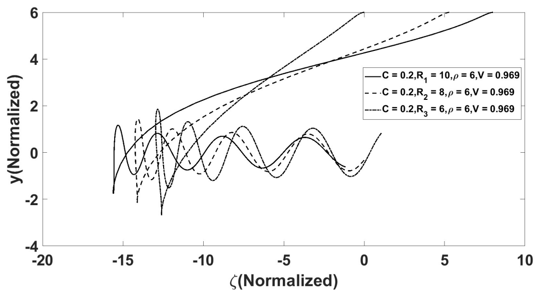


**Figure 9.** Trajectory of the electrons in longitudinal ellipsoid bubble at $C = 0.2$ and with bubble velocity $V = 0.969$ for Lorentz factor $\gamma_0 = 4$. Here the impact parameter is $\rho = 6$ with $R_1 = 10$, $R_2 = 8$, $R_3 = 6$.

spherical bubble.

### 3.3 Longitudinal phase-space of self-injected plasma electrons in different shaped bubble

In Figure 3, we have plotted longitudinal phase-space diagram of the trapped plasma electrons. Here we observe that with transverse bubble regime at $C = -0.2$ as shown in Figure 3(c), the electrons move more times than with spherical bubble at $C = 0$ as shown in Figure 3(a) and with longitudinal ellipsoid bubble at $C = 0.2$ as shown in Figure 3(b).

### 3.4 Transverse phase-space of self-injected plasma electrons in different shaped bubble

In Figure 4, after plotting the transverse phase-space of the trapped or self-injected plasma electrons, we have understood that with the transverse ellipsoid bubble at $C = -0.2$ as shown in Figure 4(c), the electrons retrace their path better than with the spherical bubble case at $C = 0$ as shown in Figure 4(a) and with the longitudinal ellipsoid bubble at $C = 0.2$ as shown in Figure 4(b).

### 3.5 Effect of impact parameter on electron trajectory

Impact parameter is defined as the radial distance between the trapped electrons and the laser pulse as the driver. If the value of the impact parameter is too small, then the trapped electrons get deflected by the generated wake. Here we consider different values of the impact parameter in different

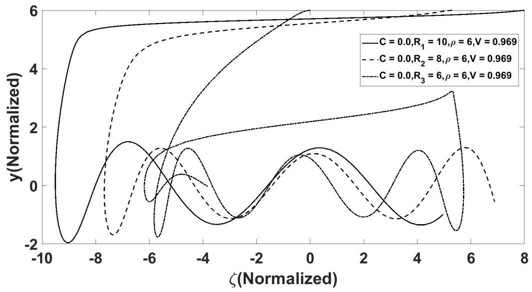


**Figure 8.** Trajectory of the electrons in spherical bubble at $C = 0.0$ and with bubble velocity $V = 0.969$ for Lorentz factor $\gamma_0 = 4$. Here the impact parameter is $\rho = 6$ with different values of bubble radius $R_1 = 10$, $R_2 = 8$, $R_3 = 6$.

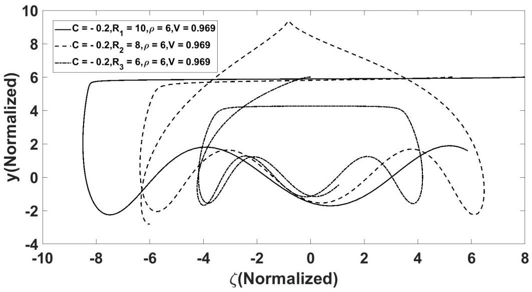


**Figure 10.** Trajectory of the electrons in transverse ellipsoid bubble at $C = -0.2$ and with bubble velocity $V = 0.969$ for Lorentz factor $\gamma_0 = 4$. Here the impact parameter is $\rho = 6$ with $R_1 = 10$, $R_2 = 8$, $R_3 = 6$.

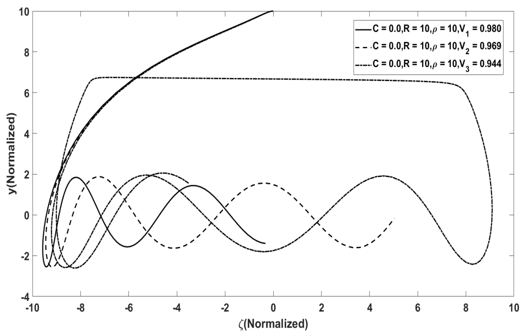


**Figure 11.** Trajectory of the electrons in spherical bubble at $C = 0.0$ with bubble radius $R = 10$ and impact parameter $\rho = 10$. Here, different bubble velocities have been considered as $V_1 = 0.980$, $V_2 = 0.969$, $V_3 = 0.944$.

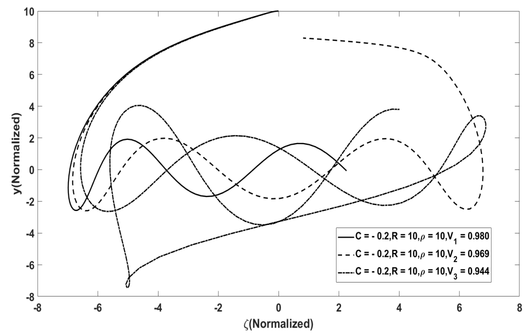


**Figure 13.** Trajectory of the electrons in transverse ellipsoid bubble at $C = -0.2$ with bubble radius $R = 10$ and impact parameter $\rho = 10$. Here, different bubble velocities have been considered as $V_1 = 0.980$, $V_2 = 0.969$, $V_3 = 0.944$.

shapes of the bubble, such as longitudinal and transverse ellipsoid shaped bubble. The impact parameter is defined as the transverse component $\rho$. We have investigated the effect of $\rho$ on spherical bubble at $C = 0.0$, longitudinal ellipsoid bubble at $C = 0.2$ and transverse ellipsoid bubble at $C = -0.2$. For these investigations, we have used three different values of the impact parameter as $\rho_1 = 10$, $\rho_2 = 8$, $\rho_3 = 6$ as shown in Figures 5, 6 and 7, respectively. We have found that with transverse ellipsoid bubble case, self-injected plasma electrons travel large distance in longitudinal as well as in transverse directions (Figure 7) as compared to the case of spherical bubble (Figure 5) and longitudinal ellipsoid bubble (Figure 6).

### 3.6 Effect of bubble radius on electron trajectory

Bubble radius is an important parameter for defining the size of the bubble. Here we have used different size of the bubble by defining different values of radius of the different shape of bubble and for this, we have first considered the spherical bubble at $C = 0.0$ with different values of bubble radius $R = R_1, R_2, R_3$. Figure 8 shows the trajectory of the electrons in spherical bubble when $R_1 = 10$, $R_2 = 8$, $R_3 = 6$ with fixed value of the bubble velocity as $V = 0.969$ and fixed impact parameter $\rho = 6$. We have found that with bubble radius $R_3 = 6$, the trapped electrons after the self-injection process move again for another self-injection process as compared to the cases of $R_1 = 10$ and $R_2 = 8$. Now for the second case, at $C = 0.2$ for longitudinal ellipsoid bubble, no second self-injection of the electrons has been seen for different size of the bubble (Figure 9). But, for the transverse ellipsoid bubble at $C = -0.2$ as shown in Figure 10, the second self-injection has been possible with different size of the bubble at $R_1 = 10$, $R_2 = 8$ and $R_3 = 6$ and this behaviour has not been possible with spherical bubble and longitudinal ellipsoid bubble.

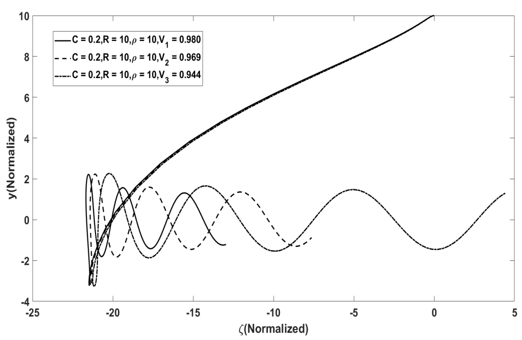


**Figure 12.** Trajectory of the electrons in longitudinal ellipsoid bubble at $C = 0.2$ with bubble radius $R = 10$ and with impact parameter $\rho = 10$. Here, different bubble velocities have been considered as $V_1 = 0.980$, $V_2 = 0.969$, $V_3 = 0.944$.

### 3.7 Effect of bubble velocity

Bubble velocity is a very important parameter for controlling the bubble shape and trapping of the electrons. We consider here different values of bubble velocity for determining the trajectory of the self-injected plasma electrons. We discuss the effect of slower bubble velocity in three different bubble shapes. For the first case, we use three different values of the bubble velocity as $V_1 = 0.980$ for $\gamma_0 = 5$, $V_2 = 0.969$ for $\gamma_0 = 4$ and $V_3 = 0.944$ for $\gamma_0 = 3$ in spherical bubble at $C = 0.0$ as shown in Figure 11. We observe that with slower bubble velocity $V_3 = 0.944$, the self-injected plasma electrons travel in larger spherical region as compared to the case with $V_1 = 0.980$ and $V_2 = 0.969$ (Figure 11) with fixed value of bubble radius $R = 10$ and impact parameter $\rho = 10$. Now for longitudinal ellipsoid bubble at $C = 0.2$, large distance is only covered in longitudinal direction at $V_3 = 0.944$ but not in transverse direction and no further self-injection has been possible for $V_3 = 0.944$ and also we observe that with $V_1 = 0.980$ and $V_2 = 0.969$, longitudinal as well as transverse distances covered by the electrons are lower (Figure 12). When the bubble shape is changed from the spherical and longitudinal ellipsoid to transverse ellipsoid at $C = -0.2$ (Figure 13), we see that the self-injected plasma electrons cover a large distance in transverse ellipsoid with slower bubble velocity with $V_3 = 0.944$ in comparison with the spherical bubble and longitudinal ellipsoid bubble. With $V_1 = 0.980$ and $V_2 = 0.969$, we find that the electrons make larger excursion in transverse ellipsoid bubble than in the spherical bubble and longitudinal ellipsoid bubble.

## 4. Conclusion

We investigated the self- injection process of the trapped plasma electrons inside different shaped bubbles named as spherical bubble, longitudinal ellipsoid bubble, and transverse ellipsoid bubble by using $4^{th}$ order Runge – Kutta method with ode45 MATLAB code. We found that the trapping is more efficient in the transverse ellipsoid bubble than the spherical bubble and the longitudinal ellipsoid bubble. We showed the plots for visualising the longitudinal and transverse phase-spaces of the trapped electrons inside the bubbles of each shape. More phase-space is found to be created in the transverse ellipsoid bubble than in the spherical and longitudinal ellipsoid bubbles, which is better for the trapped electrons for acquiring larger energy and the efficient acceleration.

**Conflict of interest statement:**
The authors declare that they have no conflict of interest.

## References


[1] T. Tajima and J. M. Dawson. "Laser electron accelerator". *Phys. Rev. Lett*, **43**:267, 1979.

[2] H. K. Malik, S. Kumar, and Y. Nishida. "Electron acceleration by laser produced wake field: Pulse shape effect". *Opt. Commun.*, **280**:417, 2007.

[3] H. K. Malik, S. Kumar, and K. P. Singh. "Electron acceleration in a rectangular waveguide filled with unmagnetized inhomogeneous cold plasma". *Laser Part. Beams*, **26**:197, 2008.

[4] K. Nakajima, A. Enomoto, H. Kobayashi, H. Nakanishi, Y. Nishida, A. Ogata, S. Ohsawa, T. Oogoe, T. Shoji, and T. Urano. "Plasma wake-field accelerator experiments at KEK". *Nucl. Instruments Methods Phys. Res. Sect. A Accel. Spectrometers, Detect. Assoc. Equip.*, **292**:12, 1990.

[5] E. Esarey, C. B. Schroeder, and W. P. Leemans. "Physics of laser-driven plasma-based electron accelerators". *Rev. Mod. Phys.*, **81**:1229, 2009.

[6] S. M. Hooker. "Developments in laser-driven plasma accelerators". *Nat. Photonics*, **7**:775, 2013.

[7] C. Joshi and T. Katsouleas. "Plasma accelerators at the energy frontier and on tabletops". *Phys. Today*, **56**:47, 2003.

[8] C. Joshi. "Plasma accelerators". *Sci. Am. 294 40–7*, **294**:40, 2006.

[9] C. Joshi. "Laser-driven plasma accelerators operating in the self-guided, blowout regime". *IEEE Trans. plasma Sci.*, **45**:3134, 2017.

[10] P. A. Norreys. "Laser-driven particle acceleration". *Nat. Photonics*, **3**:423, 2009.

[11] Y. Golian and D. Dorranian. "Proton driven plasma wakefield generation in a parabolic plasma channel". *J. Theor. Appl. Phys.*, **11**:27, 2017.

[12] I. Kostyukov, A. Pukhov, and S. Kiselev. "Phenomenological theory of laser-plasma interaction in "bubble" regime". *Phys. Plasmas*, **11**:5256, 2004.

[13] W. Lu W, C. Huang, M. Zhou, W. B. Mori, and T. Katsouleas. "Nonlinear theory for relativistic plasma wakefields in the blowout regime". *Phys. Rev. Lett.*, **96**:165002, 2006.

[14] W. Lu, C. Huang, M. Zhou, M. Tzoufras, F. S. Tsung, W. B. Mori, and T. Katsouleas. "A nonlinear theory for multidimensional relativistic plasma wave wakefields". *Phys. Plasmas*, **13**:56709, 2006.

[15] S. Kalmykov, S. A. Yi, V. Khudik, and G. Shvets. "Electron self-injection and trapping into an evolving plasma bubble". *Phys. Rev. Lett.*, **103**:135004, 2009.

[16] A. Pukhov, S. Gordienko, S. Kiselev, and I. Kostyukov. "The bubble regime of laser–plasma acceleration: monoenergetic electrons and the scalability ". *Plasma Phys. Control. fusion*, **46**:B179, 2004.

[17] S. Kumar, V. Dhaka, D. K. Singh, and H. K. Malik. "Analytical approach for the use of different gauges in bubble wakefield acceleration". *J. Theor. Appl. Phys.*, **15**:1, 2021.

[18] D. Woodbury, A. Korolov, R. Schwartz, and H. Milchberg. "Laser wakefield acceleration in the bubble regime for mid-IR laser drivers ". *APS Division of Plasma Physics Meeting Abstracts*, **133**:YO7–008, 2018.

[19] C. G. R. Geddes, C. Toth, J. Van Tilborg, E. Esarey, C. B. Schroeder, D. Bruhwiler, C. Nieter, J. Cary, and W. P. Leemans. "High-quality electron beams from a laser wakefield accelerator using plasma-channel guiding ". *Nature*, **431**:538, 2004.

[20] W. Lu, M. Tzoufras, C. Joshi, F. S. Tsung, W. B. Mori, J. Vieira, R. A. Fonseca, and L. O. Silva. "Generating multi-GeV electron bunches using single stage laser wakefield acceleration in a 3D nonlinear regime". *Phys. Rev. Spec. Top. Beams*, **10**:61301, 2007.

[21] Y. F. Li, D. Z. Li, K. Huang, M. Z. Tao, M. H. Li, J. R. Zhao, Y. Ma, X. Guo, J. G. Wang, and M. Chen. "Generation of 20 kA electron beam from a laser wakefield accelerator". *Phys. Plasmas*, **24**:23108, 2017.

[22] X. L. Xu, F. Li, W. An, T. N. Dalichaouch, P. Yu, W. Lu, C. Joshi, and W. B. Mori. "High quality electron bunch generation using a longitudinal density-tailored plasma-based accelerator in the three-dimensional blowout regime". *Phys. Rev. Accel. Beams 20 111303*, **20**:111303, 2017.

[23] J. Faure, Y. Glinec, A. Pukhov, S. Kiselev, S. Gordienko, E. Lefebvre, J. P. Rousseau, F. Burgy, and V. Malka. "A laser–plasma accelerator producing monoenergetic electron beams ". *Nature*, **431**:541, 2004.

[24] C. Gahn, G. D. Tsakiris, A. Pukhov, J. Meyer ter Vehn, G. Pretzler, P. Thirolf, D. Habs, and K. J. Witte. "Multi-MeV electron beam generation by direct laser acceleration in high-density plasma channels". *Phys. Rev. Lett.*, **83**:4772, 1999.

[25] J. Götzfried, A. Döpp, M. F. Gilljohann, F. M. Foerster, H. Ding, S. Schindler, G. Schilling, A. Buck, L. Veisz, and S. Karsch. "Physics of high-charge electron beams in laser-plasma wakefields". *Phys. Rev. X*, **10**:41015, 2020.

[26] X. Davoine, E. Lefebvre, J. Faure, C. Rechatin, A. Lifschitz, and V. Malka. "Simulation of quasimonoenergetic electron beams produced by colliding pulse wakefield acceleration". *Phys. Plasmas*, **15**:113102, 2008.

[27] H. Ekerfelt, M. Hansson, I. Gallardo González, X. Davoine, and O. Lundh. "A tunable electron beam source using trapping of electrons in a density downramp in laser wakefield acceleration". *Sci. Rep.*, **7**:1, 2017.

[28] S. Kumar, R. Dhawan, D. K. Singh, and H. K. Malik. "Diagnostic of laser wakefield acceleration with ultra–Short laser pulse by using SMILEI PIC code". *Materials Today: Proceedings*, **62**:3203, 2022.

[29] M. A. Imam, S. Jeelani, V. K. Rangari, M. G. Gome, and E. A. B. Moura. "Electron-beam irradiation effect on thermal and mechanical properties of nylon-6 nanocomposite fibers infused with diamond and diamond coated carbon nanotubes". *Int. J. Nanosci.*, **15**:1650004, 2016.

[30] A. Rousse, K. Ta Phuoc, R. Shah, A. Pukhov, E. Lefebvre, V. Malka, S. Kiselev, F. Burgy, J. P. Rousseau, D. Umstadter, and D. Hulin. "Production of a keV X-ray beam from synchrotron radiation in relativistic laser-plasma interaction". *Phys. Rev. Lett.*, **93**:1, 2004.

[31] K. T. Phuoc, F. Burgy, J. P. Rousseau, V. Malka, A. Rousse, R. Shah, D. Umstadter, A. Pukhov, and S. Kiselev. "Laser based synchrotron radiation". *Phys. Plasmas*, **12**:023101, 2005.

[32] B. Paroli and M. A. C. Potenza. "Radiation emission processes and properties: synchrotron, undulator and betatron radiation". *Adv. Phys. X*, **2**:978, 2017.

[33] E. Esarey, B. A. Shadwick, P. Catravas, and W. P. Leemans. "Synchrotron radiation from electron beams in plasma-focusing channels ". *Phys. Rev. E*, **65**:056505, 2002.

[34] H. P. Schlenvoigt, K. Haupt, A. Debus, F. Budde, O. Jäckel, S. Pfotenhauer, H. Schwoerer, E. Rohwer, J. G. Gallacher, E. Brunetti, R. P. Shanks, S. M. Wiggins, and D. A. Jaroszynski. "A compact synchrotron radiation source driven by a laser-plasma wakefield accelerator". *Nat. Phys.*, **4**:130, 2008.

[35] S. Barzegar and A. R. Niknam. " Laser pulse-electron beam synergy effect on electron self-injection and higher energy gain in laser wakefield accelerators". *Sci. Rep.*, **11**:1, 2021.

[36] R. Dhawan and H. K. Malik. "Sheath formation criterion in collisional electronegative warm plasma". *Vacuum*, **177**:109354, 2020.

[37] L. Malik, A. Escarguel, M. Kumar, A. Tevatia, and R. S. Sirohi. "Uncovering the remarkable contribution of lasers peak intensity region in holography". *Laser Phys. Lett.*, **18**:86003, 2021.

[38] L. Malik. "Tapered coils system for space propulsion with enhanced thrust: a concept of plasma detachment". *Propuls. Power Res.*, **11**:171, 2022.

[39] L. Malik and A. Escarguel. "Role of the temporal profile of femtosecond lasers of two different colours in holography". *EPL (Europhysics Lett.*, **124**:64002, 2019.

[40] H. K. Malik. *Laser-Matter Interaction for Radiation and Energy*. CRC Press, 1th edition, 2021.

[41] L. Malik. "Dark hollow lasers may be better candidates for holography". *Opt. Laser Technol.*, **132**:106485, 2020.

[42] R. Dhawan and H. K. Malik. "Modelling of electronegative collisional warm plasma for plasma-surface interaction process". *Plasma Sci. Technol.*, **23**:45402, 2021.

[43] L. Malik and A. Tevatia. "Comparative Analysis of Aerodynamic Characteristics of F16 and F22 Combat Aircraft using Computational Fluid Dynamics". *Def. Sci. J.*, **71**, 2021.

[44] L. Malik, S. Rawat, M. Kumar, and A. Tevatia. "Simulation studies on aerodynamic features of Eurofighter Typhoon and Dassault Rafale combat aircraft". *Mater. Today Proc.*, **38**:191, 2021.

[45] L. Malik, M. Kumar, and I. V. Singh. "A Three-Coil Setup for Controlled Divergence in Magnetic Nozzle ". *IEEE Trans. Plasma Sci.*, **49**:2227, 2021.

[46] R. Dhawan, M. Kumar, and H. K. Malik. "Influence of ionization on sheath structure in electropositive warm plasma carrying two-temperature electrons with non-extensive distribution". *Phys. Plasmas*, **27**:63515, 2020.

[47] I. Kostyukov, E. Nerush, A. Pukhov, and V. Seredov. "A multidimensional theory for electron trapping by a plasma wake generated in the bubble regime". *New J. Phys.*, **12**:45009, 2010.

[48] D. Lu, X. Y. Zhao, B. S. Xie, M. Ali Bake, H. B. Sang, and H.C. Wu. “Electrons trajectories around a bubble regime in intense laser plasma interaction ”. *Phys. Plasmas*, **20**:63104, 2013.

[49] E. S. Toosi, S. Mirzanejhad, and D. Dorranian. “Bubble structure in laser wake-field acceleration ”. *Laser and Particle Beams*, **34**:193, 2016.

[50] X. F. Li, Q. Yu, Y. J. Gu, S. Huang, Q. Kong, and S. Kawata. “Bubble shape and electromagnetic field in the nonlinear regime for laser wakefield acceleration”. *Phys. Plasmas*, **22**:83112, 2015.

[51] S. A. Yi, V. Khudik, S. Y. Kalmykov, and G. Shvets. “Hamiltonian analysis of electron self-injection and acceleration into an evolving plasma bubble”. *Plasma Phys. Control. Fusion*, **53**:14012, 2010.